Am J Transl Res 2023;15(2):1041-1051
www.ajtr.org /ISSN:1943-8141/AJTR0146330

Original Article

Effects of radiofrequency balloon angioplasty on the abdominal aorta in atherosclerotic rabbits

Xiaodong Xia[1,2*], Lijun Wang[2*], Pengyu Sun[1*], Yu Liu[3], Hongze Liu[4], Jiao Li[4], Qiang Chen[1], Wenfeng Shangguan[1], Weiding Wang[1], Shuai Miao[1], Tianshu Gu[1], Enzhao Liu[1], Xue Liang[1], Guangping Li[1]

[1]Tianjin Key Laboratory of Ionic-Molecular Function of Cardiovascular Disease, Department of Cardiology, Tianjin Institute of Cardiology, The Second Hospital of Tianjin Medical University, Tianjin 300211, China; [2]Department of Emergency Medicine, Tianjin Medical University General Hospital, Tianjin 300052, China; [3]Taikang Ningbo Hospital, Ningbo 315100, Zhejiang, China; [4]Department of Cardiology, Tianjin Union Medical Center, Nankai University Affiliated Hospital, Tianjin 300121, China. [*]Equal contributors.

Received September 4, 2022; Accepted January 3, 2023; Epub February 15, 2023; Published February 28, 2023

Abstract: Objectives: A novel temperature-controlled intravascular radiofrequency balloon angioplasty (RFBA) technique was designed and developed for atherosclerosis (AS) management. Methods: After establishing an AS model based on a balloon denudation injury of the abdominal aorta and a high cholesterol diet in rabbits, 46 animals were randomly assigned to the RFBA group (n = 28) or the plain balloon angioplasty (PBA) group (n = 28). The groups were further subdivided based on post-treatment euthanasia times (1 hour, 7 days, 14 days, and 28 days). Histopathological changes were observed by hematoxylin and eosin and Masson's staining. Immunohistochemistry, western blotting, and real-time quantitative polymerase chain reaction were used to detect changes in pro-inflammatory, anti-inflammatory, and apoptotic factors; TGF-β/Smad-2 pathway protein Immune levels; and mRNA levels in tissues, respectively. Results: The vascular lumen area in the RFBA group was larger than that in the PBA group at the same time points, although the change in the vascular lumen area was not different between groups. The expression of Bax, TGF-β, Smad-2, and Caspase-3 in the RFBA group was significantly higher than that in the PBA group. The expression levels of Bcl-2 in the RFBA group were significantly lower than those in the PBA group. Conclusions: At 28 days, RFBA dilated the atherosclerotic blood vessels and thickened the fibrous cap of atherosclerotic plaques to promote plaque stability. RFBA was also found to activate apoptotic factors and the TGF-/Smad-2 inflammatory pathway.

Keywords: Atherosclerosis, temperature-controlled intravascular radiofrequency balloon angioplasty, plaques, apoptotic factors

Introduction

Atherosclerosis (AS) is the main cause of cardiovascular disease and is a chronic inflammatory disease with autoimmune components [1]. Drug-eluting stents and balloon angioplasty are common clinical treatments [2]. The mechanical expansion secondary to stent and balloon placement opens the narrow arterial lumen, thereby reducing ischemic events. However, drug toxicity and mechanical damage may impair the endothelium and delay re-endothelialization, causing restenosis and very late stent thrombosis [3-5]. Therefore, alternative treatment strategies are needed.

Percutaneous transluminal angioplasty (PTA) is the primary treatment for AS. However, balloon dilation can cause mechanical damage to the arterial wall, and there is a high incidence of postoperative restenosis [6]. It is thus necessary to seek new technologies to reduce post-PTA restenosis. Studies have shown that radiofrequency can be used to anastomose blood vessels, ablate tissues and myocardium that cause arrhythmias, and recanalize occluded blood vessels completely [5, 7, 8]. *In vivo* studies have shown that radiofrequency balloon angioplasty (RFBA), which combines mechanical balloon angioplasty with radiofrequency energy, reduces restenosis compared with bal-

loon angioplasty alone [8, 9]. There are two types of radiofrequency balloon catheters, classified based on various modes of radiofrequency energy. One catheter type requires the attachment of a thin gold foil electrode to the surface of the balloon, which allows direct radiofrequency ablation on the apposed blood vessel wall [10]. The other requires the insertion of the radio frequency electrode into the balloon and heating of the liquid inside to create a thermoplastic effect during balloon expansion [11, 12]. Both techniques circumferentially heat blood vessels, which may lead to cicatricial contracture and aggravate vascular restenosis.

In this study, a novel temperature-controlled intravascular radiofrequency ablation balloon was designed. A temperature-controlled RFBA was used for longitudinal linear ablation of atherosclerotic blood vessels in rabbits, and its effect on atherosclerotic plaques was investigated. This study also investigated the changes in cytokines such as Bcl2, Bax, transforming growth factor beta (TGF-β), Smad-2, and Caspase-3 following temperature-controlled RFBA of atherosclerotic vessels, which could serve as a basis for the clinical management of AS.

Methods

Rabbit AS model

This study was approved by the Institute of Radiation Medicine of the Chinese Academy of Medical Sciences. Fifty-six healthy New Zealand purebred white rabbits, aged 3-4 months and weighing 2.5-3.5 kg, were provided by the Tianjin Yuda experimental animal breeding company of Wuqing District, Tianjin. The rabbits were acclimatized with normal feed in a room at 27°C for 2 weeks, during which they ate and drank *ad libitum*. A model of AS was constructed by feeding the rabbits a high-fat diet for 12 weeks and inducing a balloon-based intimal injury in the ventral aorta. Both groups of rabbits were randomly divided into four subgroups according to euthanasia time after treatment (1 hour, 7 days, 14 days, and 28 days), each with four rabbits.

Experimental procedure

Each rabbit was anesthetized with 3% sodium pentobarbital (1 ml/kg) through an ear-marginal vein injection, and heparin sodium 200 U/kg was administered for anticoagulation. The rabbits were fixed on the operating table, and the fur above the left femoral artery area and either the back or abdomen were shaved off. The left femoral artery was cleaned and disinfected with iodophor. Local skin anesthesia was induced using 1% lidocaine.

The skin along the femoral artery was cut approximately 4-5 cm in length to bluntly separate the subcutaneous tissue and muscle, allowing the left femoral artery to be fully exposed and freed. Two suture silk threads were used to ligate the distal end of the artery. The proximal end was clamped with a vascular clamp after sufficient dissection and separation of the 3-cm femoral artery. A small incision was made in the femoral artery to insert the indwelling needle along with a 0.014-inch guide wire, and the indwelling needle was then withdrawn at a depth of approximately 18 cm from the femoral artery rupture. Subsequently, a temperature-controlled radiofrequency balloon (3 mm) or normal balloon (3 mm) was inserted at a depth of 15 cm. The balloons with radiofrequency were inflated with a balloon pressure of 8 atm, a target temperature of 55°C, an inflation time of 30 s, and a power limit of 30 W. After rotating the catheter 180°, we applied repeated inflation with heating to the same segment, retracted the catheter by 2 cm, and repeated the procedure four times from the proximal to the distal side of the artery. The PBA group had an ordinary balloon (balloon pressure of 8 atm and inflation time of 30 s) inserted from the proximal to the distal end of the artery, and inflation was repeated four times. After the balloon was withdrawn, the artery was ligated, and the incision was sutured. Finally, the rabbits were fed with ordinary feed before their abdominal aortae were removed 1 hour, 7 days, 14 days, or 28 days after treatment.

Histological analysis

The rabbits were sacrificed 1 hour, 7 days, 14 days, or 28 days after treatment. After the abdominal aorta was removed, it was immediately rinsed in phosphate-buffered saline at 4°C and fixed with 4% neutral methanol. The tissues were fixed in formaldehyde for 24 hours and then embedded in paraffin. Deparaffinized slides were stained with hematoxylin and eosin (H&E) and Masson's stains. Finally, the slides

were sealed with neutral adhesive, observed, and photographed under the microscope.

Immunohistochemical analysis

Deparaffinized and rehydrated sections of paraffin-embedded tissue were microwaved for antigen retrieval and subsequently doused in a 3% hydrogen peroxide solution for 15 min for immunohistochemistry. After 15 min of blocking with 5% goat serum blocking buffer and overnight staining with antibodies against E-cadherin (1/200; Cell Signaling) and α-smooth muscle actin (1/100; Maixin Bio, Fujiang, China), the sections were incubated with peroxidase-conjugated secondary antibodies and 3,3'-diaminobenzidine (DAB) before being counterstained with hematoxylin. The images were viewed using an Olympus BX53 microscope and analyzed using Image J software.

RNA extraction and quantitative real-time polymerase chain reaction (qRT-PCR)

After fixing the tissues in 4% neutral methanol, they were quickly frozen in liquid nitrogen and stored at -80°C to study the expression of Bcl-2, TGF-β, Bax, Caspase-3, and Smad2 in the arterial wall. Total RNA was extracted from the abdominal aorta tissue using TRIzol reagent according to the manufacturer's instructions. The concentration and purity of the total RNA were determined using a NanoDrop ND-2000 spectrophotometer (Thermo Fisher Scientific). Denaturing agarose gel electrophoresis was used to measure RNA integrity and gDNA contamination.

The Reverse Transcription Kit (TaKaRa, Dalian, China) was used to reverse-transcribe RNA into cDNA. Glyceraldehyde 3-phosphate dehydrogenase was used as an internal control. SYBR Premix Ex Taq II (TaKaRa) was used for qRT-PCR. The $2^{-\Delta\Delta Ct}$ method was used to calculate mRNA expression in the tissues.

Western blot analysis

The cells were lysed in a radioimmunoprecipitation assay lysis solution containing phenylmethanesulfonyl fluoride, and the protein concentration was determined using the BCA Protein Assay Kit (Pierce, USA). The protein samples were separated by sodium dodecyl sulfate-polyacrylamide gel electrophoresis and transferred to polyvinylidene fluoride membranes (Millipore, USA). The membrane was blocked in 5% skimmed milk powder and incubated overnight at 4°C with the primary antibody. After washing, the membrane was incubated for 1 hour at 37°C with a secondary antibody conjugated to horseradish peroxidase. An enhanced chemiluminescence kit (Amersham, Little Chalfont, UK) was used to visualize the protein bands. ImageJ software was used to analyze the protein bands for gray values.

Statistical analysis

All statistical data were analyzed using SPSS 18.0. Data are expressed as mean ± standard deviation. Comparisons between the two groups were analyzed using paired or unpaired *t*-tests. For data with three or more groups, one-way analysis of variance (ANOVA) was used for analysis if they conformed to a normal distribution with a uniform variance; otherwise, the Kruskal-Wallis test was used. Statistical significance was set at $P < 0.05$.

Results

Construction of the AS model

Sixty rabbits were used for atherosclerosis modeling and fed a high-fat diet for 12 weeks after modeling. After 12 weeks, two rabbits had pus and ulceration at the surgical site. They did not get better with antibiotics and local debridement and eventually died. Another two rabbits were randomly sacrificed for H&E staining after 12 weeks. As shown in **Figure 1**, the model group had obvious arterial plaque formation, narrowing of the lumen, and intimal hyperplasia compared with the normal rabbit abdominal aorta, indicating that the AS model was successfully constructed.

Safety of RFBA

In the RFBA group, three rabbits expired: two died from local wound infection and one from sudden death. It was later found in the case of sudden death that there was a large amount of retroperitoneal hemorrhage and a breach in the aortic radiofrequency ablation, implying that the subject died of an aortic rupture. However, it was proven that the sudden death of the rabbit was related to radiofrequency

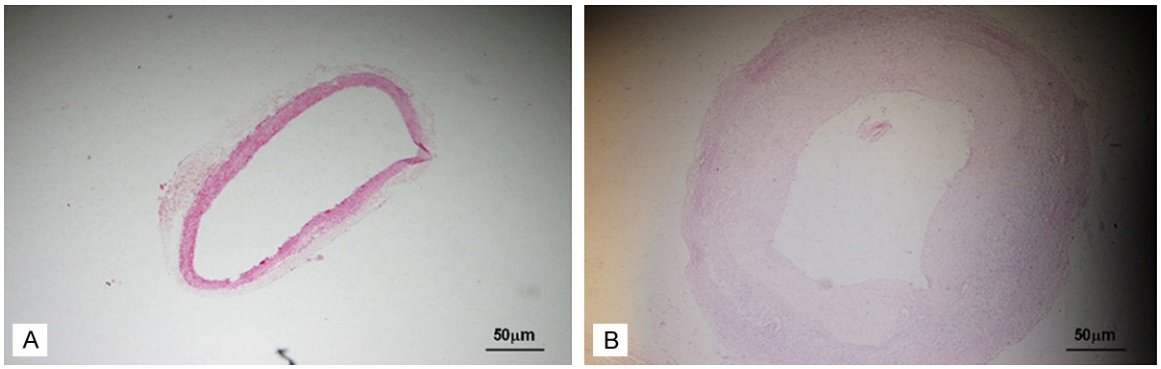

Figure 1. The abdominal aorta was pathologically stained after 12 weeks of modeling. A: Normal rabbit abdominal aorta; B: The abdominal aorta of rabbits in the model group.

Table 1. Vascular lumen area, intimal area, and tube wall thickness in each group

		Vascular lumen area (mm^2)	Intimal area (mm^2)	Tube wall thickness (mm)
PBA	1 hour	2.52 ± 0.98	3.32 ± 0.76	0.71 ± 0.09
	7 days	2.53 ± 0.94	3.55 ± 0.71	0.69 ± 0.07
	14 days	2.73 ± 0.69	3.21 ± 0.83	0.53 ± 0.14
	28 days	2.29 ± 0.72	2.92 ± 0.75	0.58 ± 0.13
RFBA	1 hour	3.58 ± 0.89	3.42 ± 1.48	0.60 ± 0.19
	7 days	3.63 ± 0.88	3.82 ± 1.53	0.61 ± 0.17
	14 days	3.62 ± 1.12	3.53 ± 1.46	0.58 ± 0.16
	28 days	3.24 ± 0.92	2.44 ± 1.10	0.48 ± 0.16

PBA: Plain Balloon Angioplasty; RFBA: Radiofrequency Balloon Angioplasty.

ablation, and further investigation into this is necessary.

Comparison of morphological parameters between the two groups

At the same time point, the temperature-controlled radiofrequency balloon group had a larger vascular lumen area than the simple balloon dilatation group ($P < 0.05$). The vascular lumen area of the two groups did not change significantly before 14 days but decreased after this time point (**Table 1**). There were no significant differences between the two groups.

Interestingly, we found that the intima area of the RFBA group did not change significantly during the first three time points (1 hour, 7 days, and 14 days). The blood vessel intima area significantly decreased at 28 days compared with the previous three time points ($P < 0.05$) (**Table 1**). Additionally, there was no statistical difference in the area of the vascular intima between the PBA and RFBA groups at the same time point ($P > 0.05$).

The tube wall thicknesses of these groups are listed in **Table 1**. The tube wall thickness of the RFBA group was smaller than that of the PBA group at 28 days ($P < 0.05$), but there was no significant difference at other time points. Moreover, the tube wall thickness of the RFBA group gradually decreased with a noticeable downward trend.

Pathological evaluation

The histopathological images are shown in **Figures 2** and **3**. The abdominal aorta tube wall was significantly thickened in the PBA group, yet the number of foam and inflammatory cells in the intima and media cell nuclei did not decrease. Contrastingly, pathological results showed that foam and inflammatory cells were observed in the intima, and vascular smooth muscle cells in the media were disordered within 1 h post-RFBA. Gradually, on the 7^{th}, 14^{th}, and 28^{th} days, the tube wall became thinner, the number of nuclei in the inner membrane as well as foam and inflammatory cells decreased, local fibrosis occurred in the inner membrane,

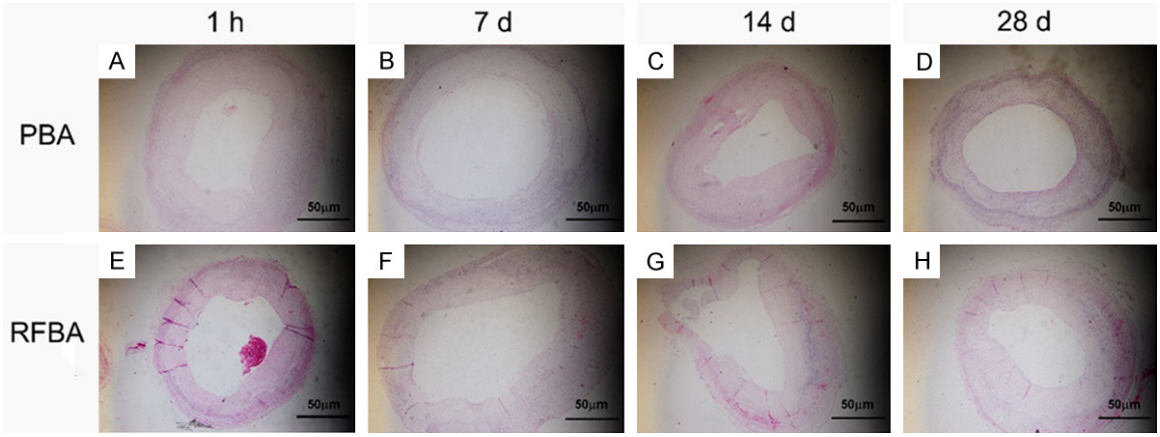

Figure 2. The representative images of hematoxylin and eosin (H&E) staining in each group. Representative images of H&E staining at 1 h (A), 7 d (B), 14 d (C), and 28 d (D) in the PBA group. Representative images of H&E staining at 1 h (E), 7 d (F), 14 d (G), and 28 d (H) in the RFBA group. PBA: Plain Balloon Angioplasty; RFBA: Radiofrequency Balloon Angioplasty.

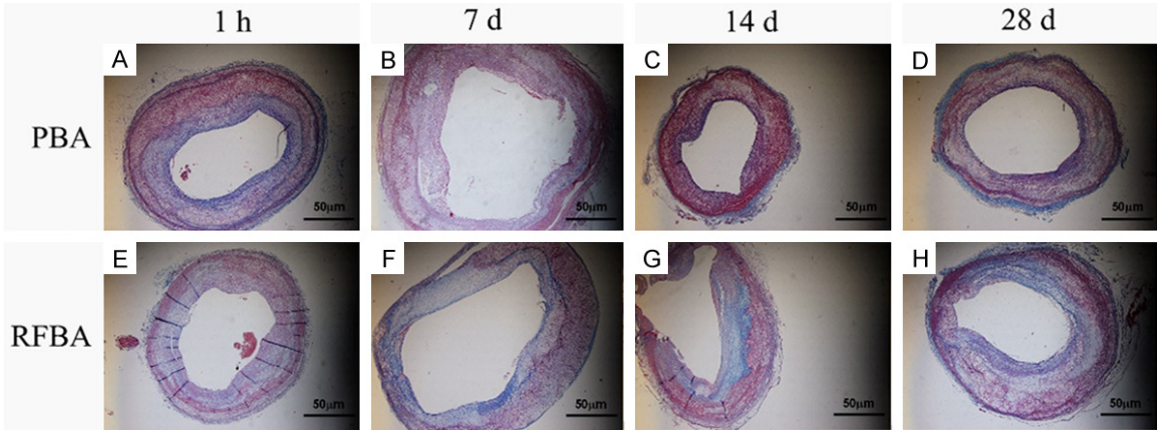

Figure 3. The representative images of Masson trichrome staining in each group. Representative images of Masson trichrome staining at 1 h (A), 7 d (B), 14 d (C), and 28 d (D) in the PBA group. Representative images of Masson trichrome staining at 1 h (E), 7 d (F), 14 d (G), and 28 d (H) in the RFBA group. PBA: Plain Balloon Angioplasty; RFBA: Radiofrequency Balloon Angioplasty.

and the smooth muscle cells of the media disappeared.

Immunohistochemistry staining for Bcl2, Bax, TGF-β, Smad2, and Caspase-3

Results showed that the expression of Bax, TGF-β, Smad-2, and Caspase-3 was higher in the RFBA group than in the PBA group, whereas the expression of Bcl-2 was lower in the RFBA group than in the PBA group (**Figure 4**). Furthermore, on the 28th day, Bax, TGF-β, Smad-2, and Caspase-3 were scattered and sporadically expressed in the PBA group, primarily in the vascular intima and middle layers, while they were expressed in all layers in the RFBA group.

Expression of Bcl-2, Bax, TGF-β, Smad2, and Caspase-3 mRNA

The mRNA expression levels of *Bcl-2*, *Bax*, *TGF-β*, *Smad2*, and *Caspase-3* are shown in **Figure 5**. The expression of *Bcl-2* in the rabbit arteries was lower in the RFBA group than in the PBA group ($P < 0.05$). However, the expression of *Bax*, *TGF-β*, *Smad2*, and *Caspase-3* was higher in the RFBA group than in the PBA group ($P < 0.05$).

Protein expression of Bcl-2, Bax, TGF-β, Smad2 and Caspase-3 in each group

The results of western blotting were consistent with those of immunochemistry. **Figure 6** shows

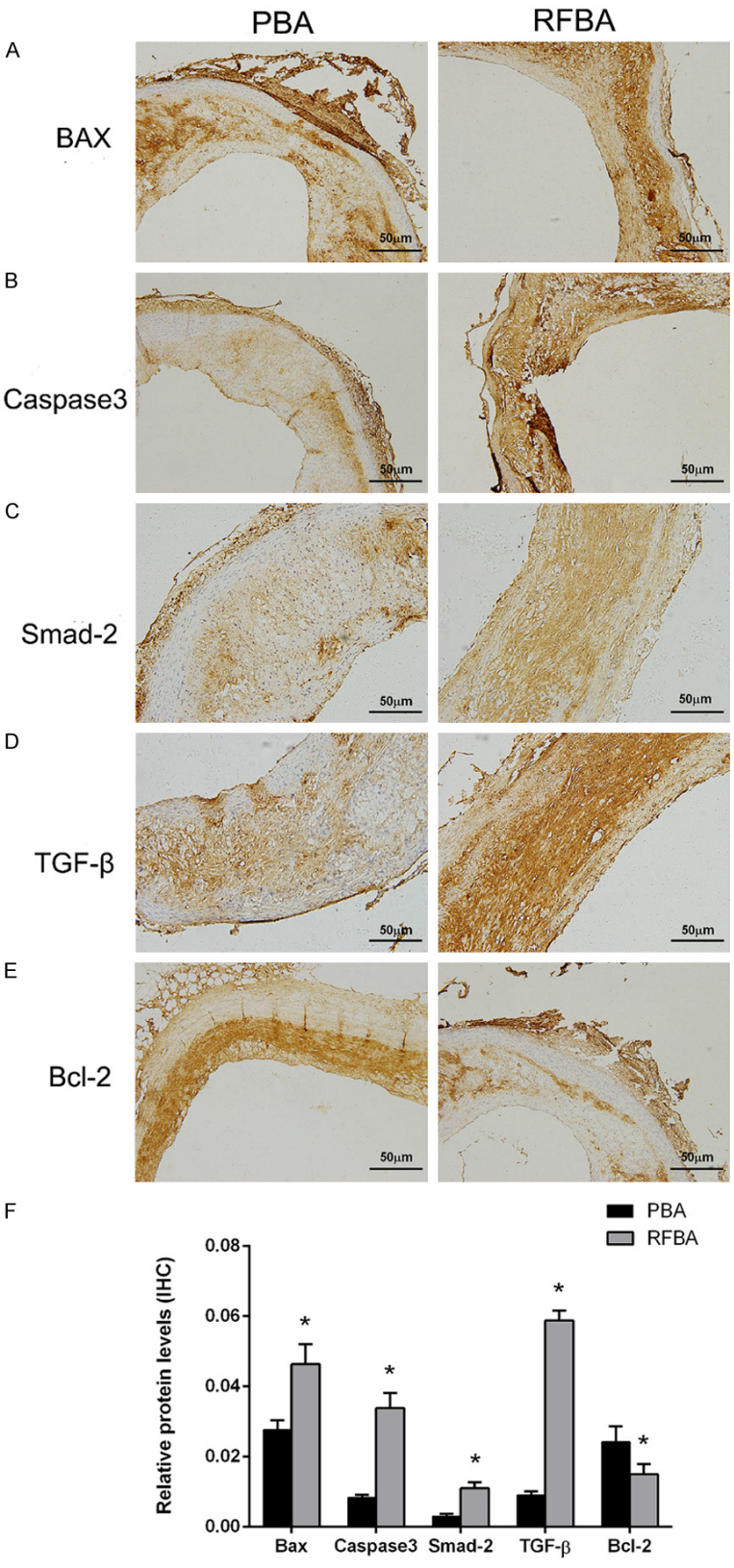

Figure 4. Immunohistochemical analyses for Bax (A), Caspase-3 (B), Smad2 (C), TGF-β (D), and Bcl-2 (E) in each group. (F) Bax, Caspase-3, Smad2, TGF-β and Bcl-2 protein expression. $^{*}P < 0.05$ versus PBA. PBA: Plain Balloon Angioplasty; RFBA: Radiofrequency Balloon Angioplasty.

protein expression levels of Bcl-2, Bax, TGF-β, Smad2, and Caspase-3. The Bcl-2 expression in the RFBA group was lower than that in the PBA group ($P < 0.05$). The RFBA group had higher levels of Bax, TGF-β, Smad2, and Caspase-3 expression than the PBA group ($P < 0.05$).

Discussion

Atherosclerosis is a systemic, lipid-driven, immune-inflammatory disease that is characterized by the appearance of multiple atherosclerotic plaques in large- and medium-sized arteries. It is the most common pathological basis for cardiovascular and cerebrovascular diseases [13, 14]. Percutaneous transluminal coronary angioplasty has been shown to improve coronary stenosis, but this can lead to complications of intravascular restenosis [15, 16]. RFBA has been proven to be a treatment for atherosclerotic arterial diseases [17, 18]. In this study, a novel temperature-controlled intravascular radiofrequency ablation balloon was designed to investigate the effects of RFBA on atherosclerotic plaques, as well as changes in apoptosis factors and TGF-/Smad-2 inflammatory pathways, to provide a new treatment approach for AS.

RFBA has a temperature dependence on the blood vessel wall [9, 19, 20]. Brasselet et al. found that local heating can significantly inhibit in-stent restenosis and neointimal hyperplasia without delaying re-endothelialization of blood vessels or increasing the risk of in-stent thrombosis after moderate heating (50°C). While high tempera-

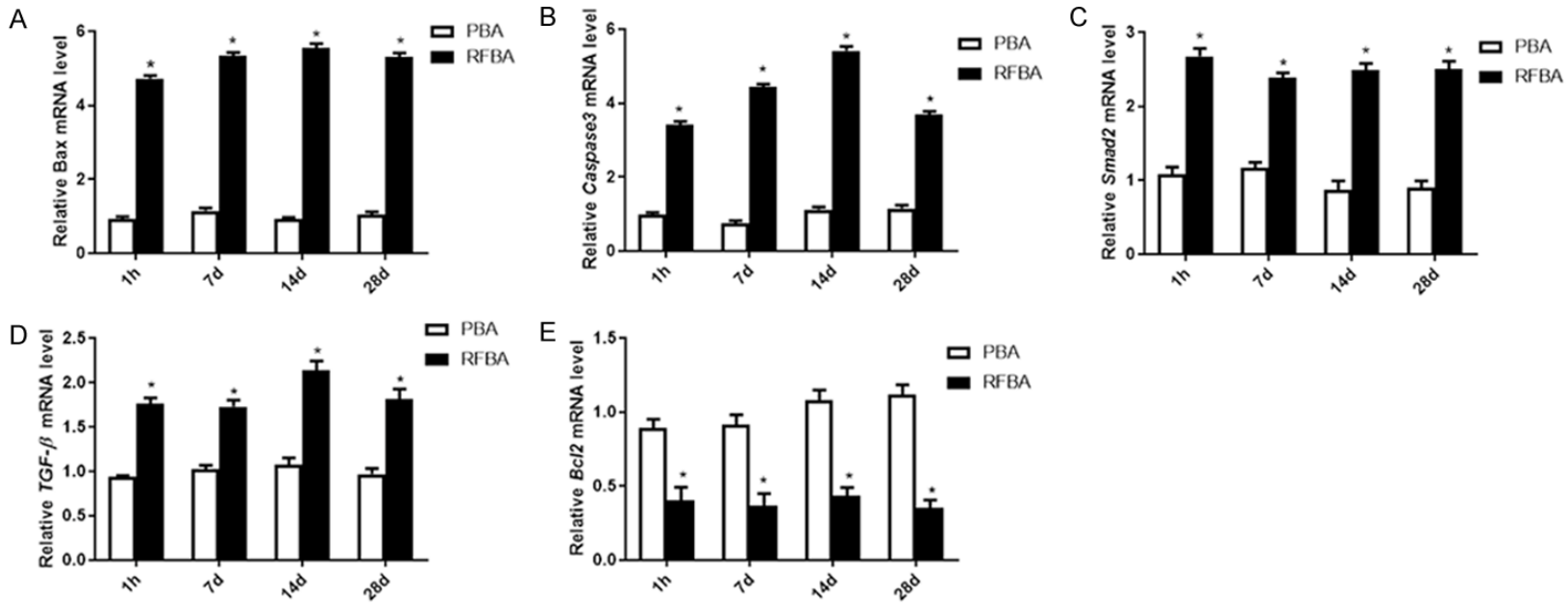

Figure 5. Expression of Bax (A), Caspase-3 (B), Smad2 (C), TGF-β (D), and Bcl-2 (E) mRNA in each group by RT-PCR. $^{*}P < 0.05$ versus PBA.

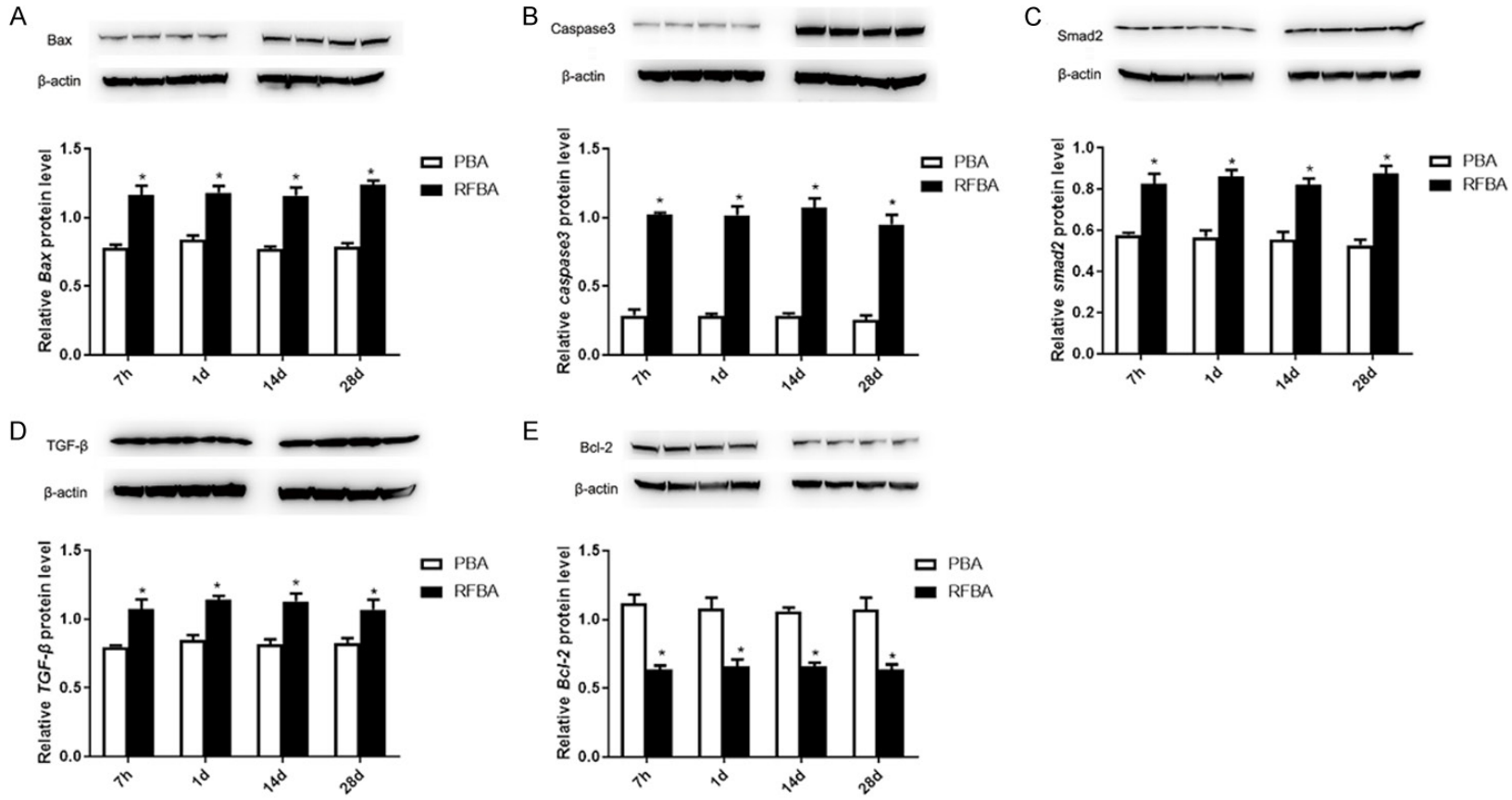

Figure 6. The protein expression of Bax (A), Caspase-3 (B), Smad2 (C), TGF-β (D), and Bcl-2 (E) in each group by Western blot. $^{*}P < 0.05$ versus PBA. PBA: Plain Balloon Angioplasty; RFBA: Radiofrequency Balloon Angioplasty.

tures (80°C and 100°C) also reduced in-stent neointimal hyperplasia, they were frequently associated with severe in-stent thrombosis. This is consistent with current study findings [11]. At a moderate temperature (55°C), the luminal area of the abdominal aorta of the rabbits in the RFBA group remained higher than that in the PBA group after 28 days.

Vascular smooth muscle cells (VSMCs) are an important component of the arterial wall, and their main functions include maintaining normal tension in the lumen and generating an extracellular matrix that constitutes the skeleton of the vessel wall [21]. VSMCs are the primary drivers of vascular pathological changes, such as intimal hyperplasia, which may occur naturally or as a result of interventional therapy [22]. This study found that the VSMC content in the vascular intima and media in the RFBA group was lower than that in the balloon dilatation group. It has been reported that the reduction of VSMC content may not be conducive to plaque stability, but the proliferation of VSMCs is associated with restenosis after coronary heart disease stenting [23-25]. In this study, it was found that although the reduction of VSMCs is not conducive to plaque stability, it may also reduce the probability of vascular restenosis. Additionally, the volume of AS plaque was reduced, and fibrous tissue proliferated due to radiofrequency injury, thus thickening the fibrous cap of an atherosclerotic plaque, which is conducive to plaque stability.

From the perspective of transcription and protein levels, the overall expression of TGF-β and Smad-2 in the rabbit arteries of the RFBA group was significantly higher than that in the PBA group. Temperature-controlled radiofrequency balloon amplification may upregulate the TGF-β/Smad signaling pathway. This may be caused by the stimulating effect of dilation on the blood vessels, which produces a stress response. Compared with PBA, RFBA has weaker stimulation of blood vessels under suitable temperatures and stimulation conditions. Therefore, the advantages of RFBA over PBA also emphasize the importance of clinically selecting suitable surgical conditions.

Moreover, immunohistochemistry evaluation showed that Bax and Caspase-3 levels were higher after RFBA than after PBA. The Bcl-2 level in the RFBA group was lower than that in the PBA group. Similar results were found for protein expression and mRNA levels. In the RFBA group, Bax and Caspase-3 levels increased, Bcl-2 levels decreased, and the Bax/Bcl-2 ratio increased. The level of apoptosis increased after RFBA dilation of the atherosclerotic plaques. Caspase-3 is the ultimate executor of apoptosis, and the Caspase-3 levels increased at the tissue or protein and transcriptional levels [26, 27]. This also suggests an increase in apoptosis, which promotes the compliance of blood vessels. Under the action of arterial blood pressure, arterial vasodilation may be maintained so that an increase in the lumen area of arterial vessels can be maintained. However, excessive apoptosis can also damage blood vessels, making them susceptible to rupture and aneurysm-like expansion [28]. Furthermore, there were a few animals that died suddenly. Necropsy revealed that the abdominal aorta was ruptured, and a large amount of blood accumulated in the retroperitoneum. This may be related to the excessive apoptosis of arterial wall cells, which is associated with the inhibition of Caspase-3 and a Bax/Bcl-2 increase. If RFBA is to be applied in clinical practice, further research on radiofrequency temperature, time, and power is needed to improve clinical safety and therapeutic effects.

This study has a few limitations. First, only the short-term outcomes from RFBA were assessed; long-term effects were not evaluated. Second, arteriography was not performed; thus, it was not possible to assess arterial vascular changes *in vivo*. Moreover, owing to the lack of imaging data, the appropriate balloon diameter was not definitively selected, which may have interfered with the study findings. Third, the results of pathological materials are relatively limited, and it was impossible to systematically and comprehensively compare molecular types and expression differences between the RFBA and PBA groups on blood vessel walls. Finally, this study did not explore the role of RFBA in stent implantation, which may limit the clinical utility of the results.

Conclusions

RFBA has the ability to increase the lumen area of the atherosclerotic blood vessels. Additionally, atherosclerotic plaques at the ablation site may undergo fibrosis, which can

help stabilize atherosclerotic plaques. However, RFBA can also activate apoptotic factors and the TGF-β/Smad-2 inflammatory pathway. Therefore, if RFBA is performed clinically, inflammatory responses must be suppressed to maintain a long-term therapeutic effect from the temperature-controlled radiofrequency balloon.

Acknowledgements

Thanks to everyone who contributed to this study. This study was supported by The National Natural Science Foundation of China Youth Science (81700304 and 82000313), The Scientific Research Fund Project of Key Laboratory of Second Hospital of Tianjin Medical University (2019ZDSYS11, 2019ZDSYS02, 2019ZDSYS10 and 2019ZDSYS07), The Foundation of Tianjin Union Medical Center (2017YJ006), The Research Fund for Central Laboratory of Second Hospital of Tianjin Medical University (2020ydey05), The Science & Technology Development Fund of Tianjin Education Commission for Higher Education (2020KJ168), Tianjin Health Research Project (No. TJWJ2022QN037), the project of China International Medical Foundation (2021-N-15-18) and Tianjin Key Medical Discipline (Specialty) Construction Project (TJYXZDXK-029A).

Disclosure of conflict of interest

None.

Address correspondence to: Guangping Li, Xue Liang and Enzhao Liu, Tianjin Key Laboratory of Ionic-Molecular Function of Cardiovascular Disease, Department of Cardiology, Tianjin Institute of Cardiology, The Second Hospital of Tianjin Medical University, Tianjin 300211, China. E-mail: tic_tjcardiol@126.com (GPL); liangxue19841219@126.com (XL); liu_ezh@126.com (EZL)

References

[1] Libby P, Buring JE, Badimon L, Hansson GK, Deanfield J, Bittencourt MS, Tokgözoğlu L and Lewis EF. Atherosclerosis. Nat Rev Dis Primers 2019; 5: 56.

[2] Levine GN, Bates ER, Blankenship JC, Bailey SR, Bittl JA, Cercek B, Chambers CE, Ellis SG, Guyton RA, Hollenberg SM, Khot UN, Lange RA, Mauri L, Mehran R, Moussa ID, Mukherjee D, Nallamothu BK and Ting HH; ACCF; AHA; SCAI. 2011 ACCF/AHA/SCAI guideline for percutaneous coronary intervention: executive summary: a report of the American College of Cardiology Foundation/American Heart Association Task Force on practice guidelines and the Society for Cardiovascular Angiography and Interventions. Circulation 2011; 124: 2574-2609.

[3] Stefanini GG and Holmes DR Jr. Drug-eluting coronary-artery stents. N Engl J Med 2013; 368: 254-265.

[4] Cassese S, Byrne RA, Tada T, Pinieck S, Joner M, Ibrahim T, King LA, Fusaro M, Laugwitz KL and Kastrati A. Incidence and predictors of restenosis after coronary stenting in 10004 patients with surveillance angiography. Heart 2014; 100: 153-159.

[5] Byrne RA, Joner M and Kastrati A. Stent thrombosis and restenosis: what have we learned and where are we going? The Andreas Grüntzig Lecture ESC 2014. Eur Heart J 2015; 36: 3320-3331.

[6] Torok RD, Campbell MJ, Fleming GA and Hill KD. Coarctation of the aorta: management from infancy to adulthood. World J Cardiol 2015; 7: 765-775.

[7] Becker GJ, Lee BI, Waller BF, Barry KJ, Kaplan J, Connolly R, Dreesen RG and Nardella P. Potential of radio-frequency balloon angioplasty: weld strengths, dose-response relationship, and correlative histology. Radiology 1990; 174: 1003-1008.

[8] Lee BI, Becker GJ, Waller BF, Barry KJ, Connolly RJ, Kaplan J, Shapiro AR and Nardella PC. Thermal compression and molding of atherosclerotic vascular tissue with use of radiofrequency energy: implications for radiofrequency balloon angioplasty. J Am Coll Cardiol 1989; 13: 1167-1175.

[9] Fram DB, Gillam LD, Aretz TA, Tangco RV, Mitchel JF, Fisher JP, Sanzobrino BW, Kiernan FJ, Nikulasson S, Fieldman A, et al. Low pressure radiofrequency balloon angioplasty: evaluation in porcine peripheral arteries. J Am Coll Cardiol 1993; 21: 1512-1521.

[10] Chenwei Jiang, Kangwei Zhang, Shiqing Zhao, Jincheng Zou, Aili Zhang and Xu LX. An RF device for effective thermal treatment of atherosclerosis. Annu Int Conf IEEE Eng Med Biol Soc 2015; 2015: 1303-1306.

[11] Brasselet C, Durand E, Addad F, Vitry F, Chatellier G, Demerens C, Lemitre M, Garnotel R, Urbain D, Bruneval P and Lafont A. Effect of local heating on restenosis and in-stent neointimal hyperplasia in the atherosclerotic rabbit model: a dose-ranging study. Eur Heart J 2008; 29: 402-412.

[12] Sreeram N, Townsend P and Morton DB. Radiofrequency thermal balloon angioplasty in an experimental model of peripheral arterial stenosis. Int J Cardiol 2000; 74: 25-32.

[13] Galkina E and Ley K. Immune and inflammatory mechanisms of atherosclerosis (*). Annu Rev Immunol 2009; 27: 165-197.
[14] Lusis AJ. Atherosclerosis. Nature 2000; 407: 233-241.
[15] Wong EM, Wu EB, Chan WW and Yu CM. A review of the management of patients after percutaneous coronary intervention. Int J Clin Pract 2006; 60: 582-589.
[16] Feldman DN, Swaminathan RV, Kaltenbach LA, Baklanov DV, Kim LK, Wong SC, Minutello RM, Messenger JC, Moussa I, Garratt KN, Piana RN, Hillegass WB, Cohen MG, Gilchrist IC and Rao SV. Adoption of radial access and comparison of outcomes to femoral access in percutaneous coronary intervention: an updated report from the national cardiovascular data registry (2007-2012). Circulation 2013; 127: 2295-2306.
[17] Li L, Wang R, Shi HH, Xie L, Li JD, Kong WC, Tang JT, Ke DN and Zhao LY. In vitro study on the feasibility of magnetic stent hyperthermia for the treatment of cardiovascular restenosis. Exp Ther Med 2013; 6: 347-354.
[18] Orihara K, Biro S, Hamasaki S, Eto H, Miyata M, Ikeda Y and Tei C. Hyperthermia at 43 degrees C for 2 h inhibits the proliferation of vascular smooth muscle cells, but not endothelial cells. J Mol Cell Cardiol 2002; 34: 1205-1215.
[19] Fram DB, Aretz TA, Mikan JF, Raisner A, Mitchel JF, Gillam LD, Waters DD and McKay RG. In vivo radiofrequency thermal balloon angioplasty of porcine coronary arteries: histologic effects and safety. Am Heart J 1993; 126: 969-978.
[20] Douek PC, Correa R, Neville R, Unger EF, Shou M, Banai S, Ferrans VJ, Epstein SE, Leon MB and Bonner RF. Dose-dependent smooth muscle cell proliferation induced by thermal injury with pulsed infrared lasers. Circulation 1992; 86: 1249-1256.
[21] Wagenseil JE and Mecham RP. Vascular extracellular matrix and arterial mechanics. Physiol Rev 2009; 89: 957-989.
[22] Bennett MR, Sinha S and Owens GK. Vascular smooth muscle cells in atherosclerosis. Circ Res 2016; 118: 692-702.
[23] Marx SO, Totary-Jain H and Marks AR. Vascular smooth muscle cell proliferation in restenosis. Circ Cardiovasc Interv 2011; 4: 104-111.
[24] Schillinger M and Minar E. Percutaneous treatment of peripheral artery disease: novel techniques. Circulation 2012; 126: 2433-2440.
[25] Finn AV, Nakano M, Narula J, Kolodgie FD and Virmani R. Concept of vulnerable/unstable plaque. Arterioscler Thromb Vasc Biol 2010; 30: 1282-1292.
[26] Yang B, El Nahas AM, Thomas GL, Haylor JL, Watson PF, Wagner B and Johnson TS. Caspase-3 and apoptosis in experimental chronic renal scarring. Kidney Int 2001; 60: 1765-1776.
[27] Shang N, Bank T, Ding X, Breslin P, Li J, Shi B and Qiu W. Caspase-3 suppresses diethylnitrosamine-induced hepatocyte death, compensatory proliferation and hepatocarcinogenesis through inhibiting p38 activation. Cell Death Dis 2018; 9: 558.
[28] Choke E, Cockerill G, Wilson WR, Sayed S, Dawson J, Loftus I and Thompson MM. A review of biological factors implicated in abdominal aortic aneurysm rupture. Eur J Vasc Endovasc Surg 2005; 30: 227-244.